

AD-A048 969

AIR FORCE INST OF TECH WRIGHT-PATTERSON AFB OHIO SCH--ETC F/G 20/5
KINETICS AND WAVE LENGTH DEPENDENCE OF THE PHOTOLYTIC DEGRADATI--ETC(U)
DEC 77 K O'BRIEN

UNCLASSIFIED

AFIT/GEP/AA/77D-2

NL

| OF |

ADAO48969



END
DATE
FILMED
2 - 78
DDC

AD A 048969

AD No. ~~1~~
DDC FILE COPY



12



DDC
JAN 23 1978
F

UNITED STATES AIR FORCE
AIR UNIVERSITY
AIR FORCE INSTITUTE OF TECHNOLOGY
Wright-Patterson Air Force Base, Ohio

DISTRIBUTION STATEMENT A
Approved for public release;
Distribution Unlimited

①



**KINETICS AND WAVE LENGTH DEPENDENCE
OF THE PHOTOLYTIC DEGRADATION OF
KITON RED-S LASER DYE**

THESIS

AFIT/GEP/AA/77D-2

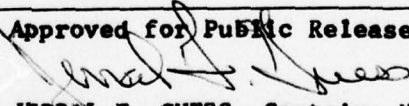
**Kevin O'Brien
2 Lt USAF**

Approved for public release; distribution unlimited

UNCLASSIFIED

SECURITY CLASSIFICATION OF THIS PAGE (When Data Entered)

UNCLASSIFIED

REPORT DOCUMENTATION PAGE		READ INSTRUCTIONS BEFORE COMPLETING FORM
1. REPORT NUMBER AFIT/GEP/AA/77D-2 ✓	2. GOVT ACCESSION NO.	3. RECIPIENT'S CATALOG NUMBER
4. TITLE (and Subtitle) KINETICS AND WAVE LENGTH DEPENDENCE OF THE PHOTOLYTIC DEGRADATION OF KITON RED-S LASER DYE		5. TYPE OF REPORT & PERIOD COVERED AFIT Thesis
7. AUTHOR(s) Kevin O'Brien 2Lt USAF		6. PERFORMING ORG. REPORT NUMBER
9. PERFORMING ORGANIZATION NAME AND ADDRESS Air Force Institute of Technology (AFIT-EN) ✓ Wright-Patterson AFB, OH 45433		8. CONTRACT OR GRANT NUMBER(s)
11. CONTROLLING OFFICE NAME AND ADDRESS		10. PROGRAM ELEMENT, PROJECT, TASK AREA & WORK UNIT NUMBERS Project 2001 01 54
14. MONITORING AGENCY NAME & ADDRESS (if different from Controlling Office)		12. REPORT DATE December 1977
		13. NUMBER OF PAGES 57
		15. SECURITY CLASS. (of this report) UNCLASSIFIED
		15a. DECLASSIFICATION/DOWNGRADING SCHEDULE
16. DISTRIBUTION STATEMENT (of this Report) Approved for public release; distribution unlimited		
17. DISTRIBUTION STATEMENT (of the abstract entered in Block 20, if different from Report)		
18. SUPPLEMENTARY NOTES Approved for Public Release IAW AFR 190-17  JERRAL F. GUESS, Captain, USAF Director of Information		
19. KEY WORDS (Continue on reverse side if necessary and identify by block number) Dye Dye Laser Photodegradation Reaction Kinetics		
20. ABSTRACT (Continue on reverse side if necessary and identify by block number) The laser dye Kiton Red-S in ethanol was degraded using continuous radiation and pulsed radiation from the flash lamp of a dye laser. Data from infrared spectrograms was used to construct plots of the concentration of Kiton Red-S versus the time of exposure. From these plots the rate equation was determined. The effect on the rate of reaction of different oxygen concentrations was observed. Qualitative information from the infrared spectra was used to identify photo products. The fluorescence and power were monitored during the pulsed laser experiment to determine the primary effect of the photo products. The reaction was found to		

UNCLASSIFIED

SECURITY CLASSIFICATION OF THIS PAGE (When Data Entered)

Continuation of Block 20. ABSTRACT

be zeroth order in Kiton Red-S and the presence of oxygen accelerates the reaction. The products were found to be esters and carboxylic acids. The effect of the products on the laser was to absorb the pump radiation.

1. REPORT NUMBER	2. REPORT DATE	3. REPORT TYPE AND PERIOD	4. AUTHOR
5. PERFORMING ORG. REPORT NUMBER	6. CONTRACT OR GRANT NUMBER(s)	7. PROGRAM ELEMENT PROJECT, TASK AREA & WORK UNIT NUMBERS	8. PERFORMING ORGANIZATION NAME AND ADDRESS
9. CONTROLLING OFFICE NAME AND ADDRESS	10. MONITORING AGENCY NAME & ADDRESS (if different from Controlling Office)	11. SECURITY CLASS. (of this report)	12. DISTRIBUTION STATEMENT (of this Report)
13. NUMBER OF PAGES	14. REPORT DATE	15. SECURITY CLASS. (of this report)	16. DISTRIBUTION STATEMENT (of this Report)
17. NUMBER OF PAGES	18. REPORT DATE	19. SECURITY CLASS. (of this report)	20. DISTRIBUTION STATEMENT (of this Report)
21. NUMBER OF PAGES	22. REPORT DATE	23. SECURITY CLASS. (of this report)	24. DISTRIBUTION STATEMENT (of this Report)
25. NUMBER OF PAGES	26. REPORT DATE	27. SECURITY CLASS. (of this report)	28. DISTRIBUTION STATEMENT (of this Report)
29. NUMBER OF PAGES	30. REPORT DATE	31. SECURITY CLASS. (of this report)	32. DISTRIBUTION STATEMENT (of this Report)
33. NUMBER OF PAGES	34. REPORT DATE	35. SECURITY CLASS. (of this report)	36. DISTRIBUTION STATEMENT (of this Report)
37. NUMBER OF PAGES	38. REPORT DATE	39. SECURITY CLASS. (of this report)	40. DISTRIBUTION STATEMENT (of this Report)
41. NUMBER OF PAGES	42. REPORT DATE	43. SECURITY CLASS. (of this report)	44. DISTRIBUTION STATEMENT (of this Report)
45. NUMBER OF PAGES	46. REPORT DATE	47. SECURITY CLASS. (of this report)	48. DISTRIBUTION STATEMENT (of this Report)
49. NUMBER OF PAGES	50. REPORT DATE	51. SECURITY CLASS. (of this report)	52. DISTRIBUTION STATEMENT (of this Report)
53. NUMBER OF PAGES	54. REPORT DATE	55. SECURITY CLASS. (of this report)	56. DISTRIBUTION STATEMENT (of this Report)
57. NUMBER OF PAGES	58. REPORT DATE	59. SECURITY CLASS. (of this report)	60. DISTRIBUTION STATEMENT (of this Report)
61. NUMBER OF PAGES	62. REPORT DATE	63. SECURITY CLASS. (of this report)	64. DISTRIBUTION STATEMENT (of this Report)
65. NUMBER OF PAGES	66. REPORT DATE	67. SECURITY CLASS. (of this report)	68. DISTRIBUTION STATEMENT (of this Report)
69. NUMBER OF PAGES	70. REPORT DATE	71. SECURITY CLASS. (of this report)	72. DISTRIBUTION STATEMENT (of this Report)
73. NUMBER OF PAGES	74. REPORT DATE	75. SECURITY CLASS. (of this report)	76. DISTRIBUTION STATEMENT (of this Report)
77. NUMBER OF PAGES	78. REPORT DATE	79. SECURITY CLASS. (of this report)	80. DISTRIBUTION STATEMENT (of this Report)
81. NUMBER OF PAGES	82. REPORT DATE	83. SECURITY CLASS. (of this report)	84. DISTRIBUTION STATEMENT (of this Report)
85. NUMBER OF PAGES	86. REPORT DATE	87. SECURITY CLASS. (of this report)	88. DISTRIBUTION STATEMENT (of this Report)
89. NUMBER OF PAGES	90. REPORT DATE	91. SECURITY CLASS. (of this report)	92. DISTRIBUTION STATEMENT (of this Report)
93. NUMBER OF PAGES	94. REPORT DATE	95. SECURITY CLASS. (of this report)	96. DISTRIBUTION STATEMENT (of this Report)
97. NUMBER OF PAGES	98. REPORT DATE	99. SECURITY CLASS. (of this report)	100. DISTRIBUTION STATEMENT (of this Report)

Approved for public release; distribution unlimited

Approved for Public Release IAW AFR 190-17

JERRAL F. GUESS, Captain, USAF
Director of Information

The laser dye Kiton Red-S in ethanol was degraded using continuous radiation and pulsed radiation from the flash lamp of a dye laser. Data from infrared spectrograms was used to construct plots of the concentration of Kiton Red-S versus the time of exposure. From these plots the rate equation was determined. The effect on the rate of reaction of different oxygen concentrations was observed. Qualitative information from the infrared spectra was used to identify photo products. The fluorescence and power were monitored during the pulsed laser experiment to determine the primary effect of the photo products. The reaction was found to

UNCLASSIFIED

14

AFIT/GEP/AA/77D-2

6

KINETICS AND WAVE LENGTH DEPENDENCE
OF THE PHOTOLYTIC DEGRADATION OF
KITON RED-S LASER DYE.

9

Master's THESIS

Presented to the Faculty of the School of Engineering
of the Air Force Institute of Technology
Air University
in Partial Fulfillment of the
Requirements for the Degree of
Master of Science

62204F

16

2001

17

01

12 61p.

10

by

Kevin O'Brien B.S.

2 Lt

USAF

Graduate Engineering Physics

11

December 1977

APPROVED FOR	
NO IS	Active Section <input checked="" type="checkbox"/>
DOC	Ref Section <input type="checkbox"/>
UNCLASSIFIED	<input type="checkbox"/>
by	
DISTRIBUTION/AVAILABILITY CODES	
1. 2. 3. 4. 5. 6. 7. 8. 9. 10. 11. 12. 13. 14. 15. 16. 17. 18. 19. 20. 21. 22. 23. 24. 25. 26. 27. 28. 29. 30. 31. 32. 33. 34. 35. 36. 37. 38. 39. 40. 41. 42. 43. 44. 45. 46. 47. 48. 49. 50. 51. 52. 53. 54. 55. 56. 57. 58. 59. 60. 61. 62. 63. 64. 65. 66. 67. 68. 69. 70. 71. 72. 73. 74. 75. 76. 77. 78. 79. 80. 81. 82. 83. 84. 85. 86. 87. 88. 89. 90. 91. 92. 93. 94. 95. 96. 97. 98. 99. 100.	
A	

Approved for public release; distribution unlimited

012 225

LB

Preface

It is hoped that this thesis will make a real contribution to the understanding of the photolysis of the xanthene dyes. There are many people whom I would like to thank for their help on this project. First, I would like to thank my advisor, Dr. Ernest A. Dorko, for his excellent help, advice, suggestions and encouragement on this project. I would like to thank the personnel at the Air Force Avionics Laboratory, Capt Sidney Johnson, Lt Gary Smith, and Mr. Frank Kile for their extensive help. I would like to thank Mr. William Baker and Mr. Robert Wade for their help in building equipment and obtaining supplies. I would also like to thank Lt Randall Rushe for his help in computations. Finally, I would like to thank Mrs. Frances Jarnagin who typed this thesis.

Kevin O'Brien

Contents

	<u>Page</u>
Preface	ii
List of Figures	v
List of Tables	vi
List of Symbols	vii
Abstract	ix
I. Introduction	1
Justification	1
Objectives	1
Experimental Approach	2
Assumptions	3
II. Theory	4
Quantum Mechanics of Dyes	4
Dye Solution Degradation	6
Infrared Spectroscopy	7
Reaction Kinetics	8
Power Output of a Laser	9
III. Apparatus	10
Continuous Radiation Photolysis System	10
Dye Laser System	13
Analysis Equipment	17
IV. Experimental Procedure	18
Continuous Radiation Photolysis	18
Flash Photolysis	18
Sample Analysis	19
Experimental Details	20
V. Data Reduction	21
VI. Results	23
Qualitative Results	23
Quantitative Results	23

VII.	Discussion	31
	Discussion of CW Photolysis Results	31
	Discussion of Laser Results	34
VIII.	Conclusions	35
IX.	Recommendations	36
	Bibliography	37
	Appendix A: Sample Calculation	39
	Appendix B: Tabular Data	43
	VITA	48

List of Figures

<u>Figure</u>		<u>Page</u>
1	Structure of Kiton Red-S	5
2	Energy Level Diagram	5
3	The Photolysis System	11
4	Spectrum of the Lamp	12
5	The Dye Container	12
6	Types of Lasers	14
7	Schematic of the Dye Laser	15
8	Fluorescence Measuring Equipment	16
9	Fluorescence of Kiton Red-S in Ethanol	22
10	IR Spectrum of Kiton Red-S	24
11	IR Spectrum of Degraded Kiton Red-S	24
12	Calibration Curve	26
13	Degradation of KRS, Zero Oxygen	28
14	Degradation of KRS, 10.3 Percent Oxygen	28
15	Degradation of KRS, 21 Percent Oxygen	29
16	IR Spectrum of Partially Degraded Kiton Red-S	41
17	Conversion Scale for Transmittance to Absorbance	42

List of Tables

<u>Table</u>		<u>Page</u>
I	Infrared Assignments	25
II	Numerical Results	34
III	Data from The Calibration Curve	44
IV	Data from Trial One	45
V	Data from Trial Two	46
VI	Data from Trial Three	47

List of Symbols

Symbol

a	Experimentally determined number
A	Absorbance at peak
A_0	Absorbance at tie line
C	Concentration, Moles/liter
I	Intensity
I_0	Incident intensity
k	Actual rate constant, Mole/liter sec
K	Apparent rate constant, Mole/liter sec
K_H	Henry's law constant, Atmospheres
K_{laser}	Laser rate constant
l	Distance through medium
L	Length of laser medium
P	Partial pressure, Atmospheres
P_{fluor}	Fluorescence power
P_{laser}	Laser output power, Watts
r	Correlation coefficient
r_1	Reflectivity of mirror one
r_2	Reflectivity of mirror two
R_p	Pump rate for laser
$R_{p \text{ th}}$	Pump rate for laser at threshold
S_0	Ground state of dye molecule
S_1	First excited singlet state of dye molecule
t	Time, Hour

Symbol

T_1	First excited triplet state of dye molecule
T_2	Second excited triplet state of dye molecule
X	Chemical species
X	Mole fraction
α	Absorption coefficient
α_0	Absorption coefficient of laser medium
τ_c	Photon cavity lifetime
τ_2	Lifetime of the upper laser level

Abstract

The laser dye Kiton Red-S in ethanol was degraded using continuous radiation and pulsed radiation from the flash lamp of a dye laser. Data from infrared spectrograms was used to construct plots of the concentration of Kiton Red-S versus the time of exposure. From these plots the rate equation was determined. The effect on the rate of reaction of different oxygen concentrations was observed. Qualitative information from the infrared spectra was used to identify photo products. The fluorescence and power were monitored during the pulsed laser experiment to determine the primary effect of the photo products. The reaction was found to be zeroth order in Kiton Red-S and the presence of oxygen accelerates the reaction. The products were found to be esters and carboxylic acids. The effect of the products on the laser was to absorb the pump radiation.

KINETICS AND WAVE LENGTH DEPENDENCE
OF THE PHOTOLYTIC DEGRADATION OF
KITON RED-S LASER DYE

I. Introduction

Justification

Dyes are one of the latest materials that have exhibited lasing ability. The property that makes dyes attractive is their easy wide-range tunability. Dye lasers are also attractive because they span the spectrum from the near infrared (IR) to the near ultraviolet (UV) and exhibit medium energies and powers at excellent efficiencies. Among the problems that limit the usefulness of these lasers is that the power or energy output decreases drastically with use due to photolytic degradation of the dyes.

Objectives

The primary objective of this investigation was to study the photolytic degradation of Kiton Red-S (KRS) in ethanol, and to find ways of slowing or eliminating the degradation primarily through filtering of the laser pump radiation. This study was to be done in two ways, continuous (cw) radiation from a 200 watt mercury point source and pulsed radiation from a Xenon flash lamp in an actual dye laser.

The secondary objectives were to assemble and demonstrate a working dye laser system, and to refine the method used to analyze the degradation.

Kiton Red-S was chosen as the dye solution because it represents a family of very common laser dyes, the xanthenes. Other members of this family include the Rhodamines. The solvent used was ethanol. A fairly polar solvent like ethanol was needed because KRS is a polar molecule. A more polar solvent than ethanol was not used to prevent aggregation of the dye molecules (Ref 5:158-160).

Experimental Approach

There were two experiments run, continuous radiation photolysis and flash photolysis. In the continuous radiation photolysis experiment the dye solution was placed in a container whose bottom half was quartz. A quantity of the dye solution was placed in the container and the photolysis system was assembled. The system and the solution were equilibrated with a chosen gas mixture by bubbling the desired gas mixture through the dye solution. The dye was exposed to the radiation and samples of the dye were taken during the run. These samples were analyzed by IR spectroscopy.

In the flash photolysis experiment the dye solution was photolyzed in a triaxial dye laser system. The initial power and the fluorescence spectrum were measured. After a certain number of pulses the power and the fluorescence spectrum were measured again.

Infrared spectroscopy was chosen as the primary method of analysis because it yields both qualitative and quantitative data. An IR spectrum of a compound serves as a "fingerprint" of that compound (Ref 2:199). If the structure of the compound changes, the spectrum changes. The intensity of the spectrum gives the amount of the compound in the solution.

Assumptions

The most critical assumptions made were that the output of the mercury lamp and the output of the flash lamp were constant. The Beer Lambert law was assumed to hold at the concentrations used. Other assumptions are mentioned in the text.

II. Theory

Quantum Mechanics of Dyes

Kiton Red-S whose structure is shown in Fig. 1 is an efficient laser dye from 589 nm to 642 nm (Ref 15:346). The dye has an electronic energy level structure that is typical of conjugated organic molecules. The most important levels for laser work are shown in Fig. 2. The ground state is S_0 , S_1 is the first excited singlet state, T_1 is the first excited triplet state, and T_2 is the second excited triplet state. Each of these levels is a quasi-continuum due to numerous close splitting of the levels by vibrational and rotational states (Ref 13:650).

The dye laser is a classical four level laser system. During pumping, electrons are excited from S_0 to one of the upper vibrational levels of S_1 . The molecules relax nonradiatively to the lowest vibrational level of S_1 . The laser transition is the radiative transition from the lowest vibrational level of S_1 to one of the upper vibrational levels of S_0 . Finally the molecules relax to the lowest vibrational level of S_0 nonradiatively (Ref 13:650-653).

There are a number of competing pathways possible. First the transition from T_1 to T_2 lies in the same energy range as the transition from S_0 to S_1 . The T_1 to T_2 transition therefore competes for pump radiation. A pathway that competes with the laser transition is the nonradiative transition from S_1 to T_1 . This is known as intersystem crossing. The radiative transition from T_1 to S_0 is forbidden and has a large time constant. As a consequence, dye solutions with a large

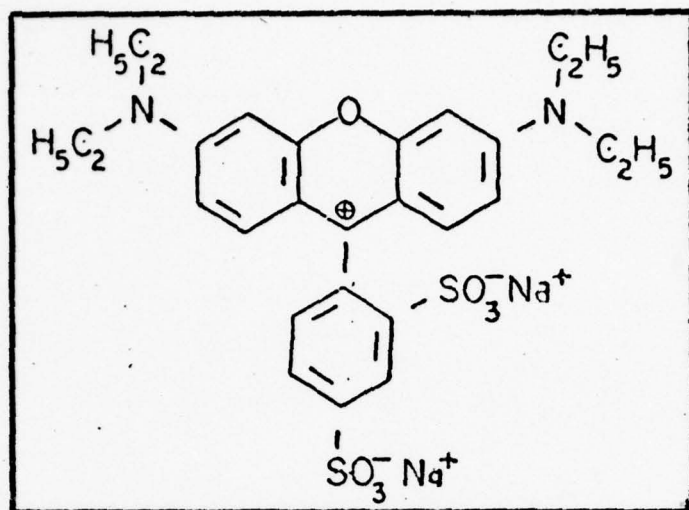


Fig. 1. Structure of Kiton Red-S

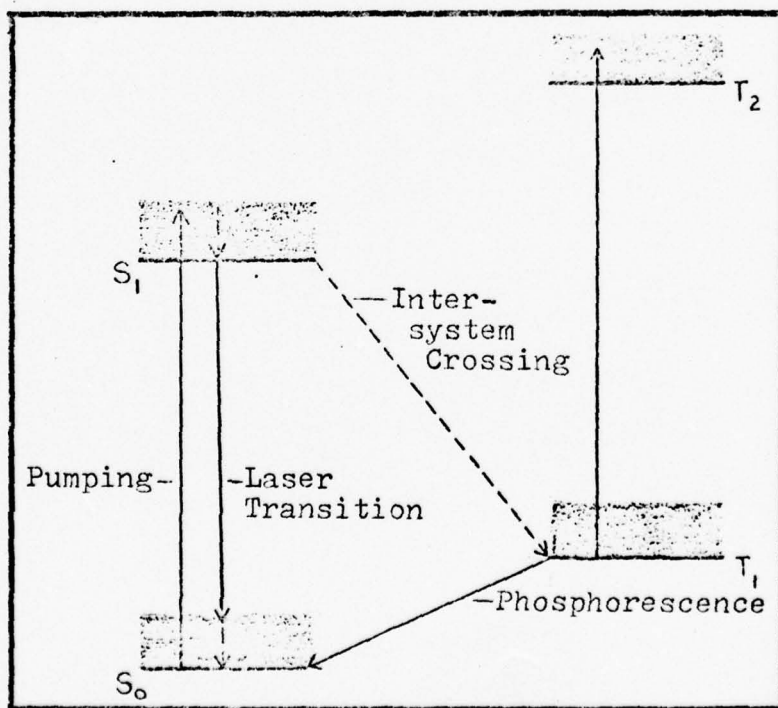


Fig. 2. Energy Level Diagram

intersystem crossing rate tend to have their molecules pile up in the T_1 state leaving few molecules available to lase (Ref 13:653).

Dye Solution Degradation

There have been many studies on degradation of various dye solutions. The degradation has been found to be permanent and due primarily to the flash lamp radiation (Ref 19:723). For KRS in ethanol the portion of the flash lamp radiation that causes the damage lies in the UV (Ref 12:36). The rate of degradation is strongly dependent on the wavelength of the incident radiation (Ref 18:35). The rate of degradation also depends linearly on the output power of the flash lamp, and the volume of the solution (Ref 8:178 and 12:36).

It is fairly well agreed upon that the effect of the photochemical products formed in the photolysis is either to compete for pump radiation or to absorb the stimulated radiation (Ref 11:1126). The photochemical products may arise from three sources: the solvent, the dye, or a combination of the dye and the solvent (Ref 19:723, 11:1126, and 20:94).

The role of oxygen in the photolysis of dye solutions has been ambiguous. In one paper on rhodamine 6G in methanol it was shown that the presence of oxygen slows the degradation (Ref 9:329). On the other hand an earlier paper on the same solution shows an increase in the rate of degradation in the presence of oxygen (Ref 3:308).

Oxygen can act in two ways in a dye solution. First it can act as a triplet quencher, in which oxygen increases the rate of the T_1 to S_0 transition by collisions with the dye molecule. Since the triplet state is an excited form of the molecule, oxygen might serve to stabilize the

dye by reducing the number of molecules in the triplet state. On the other hand oxygen may act as a reactant in a photochemical oxidation reaction and hence will be a destabilizing agent.

Infrared Spectroscopy

The portion of the electromagnetic spectrum that corresponds to the energies involved in bending and stretching a chemical bond lie in the IR. Each type of chemical bond between various atoms has its own energy. The resonant frequency of a particular normal mode of vibration for that bond depends on the bond energy and the mass of the atoms attached. For various types of bonds between various atoms each with their own mass there is a unique resonant frequency for each normal mode of vibration. The situation for a large molecule is complex due to the fact that there is coupling from all parts of the molecule (Ref 2:197-203).

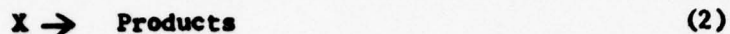
If IR radiation were passed through some group of molecules, the portions of the IR spectrum that corresponded to a resonant mode would be absorbed according to the laws of quantum mechanics. The amount of radiation absorbed would depend on the quantum efficiency of the mode excited and the number of molecules encountered. The strength of the absorption is given by Beer's law

$$I = I_0 e^{-\alpha C l} \quad (1)$$

I_0 is the intensity of the incident radiation, I is the intensity after passing through the medium a distance of l , α is some constant related to the quantum efficiency of the absorption, and C is the concentration of the solution (Ref 2:799).

Reaction Kinetics

For a simple decomposition reaction



the appropriate rate equation would be

$$\frac{d[X]}{dt} = -K[X]^a \quad (3)$$

where the brackets indicate concentration, and a is some constant known as the order of the reaction. The most common values for a are zero, one, and two. If a equals two, Eq (3) is a second order rate equation. If the equation is then integrated, the resulting equation is

$$\frac{1}{[X]} = -Kt + \text{Const} \quad (4)$$

If $\frac{1}{[X]}$ versus t is plotted, the plot would be a straight line.

If a equals one, Eq (3) is a first order rate equation. When integrated the equation yields

$$\ln [X] = -Kt + \text{Const} \quad (5)$$

A plot of $\ln [X]$ versus t would give a straight line.

If a equals zero, Eq (3) is a zeroth order rate equation. When integrated the equation would give

$$[X] = -Kt + \text{Const} \quad (6)$$

A plot of $[X]$ versus t would yield a straight line (Ref 1:617-624).

The amount of any particular gas dissolved in a liquid under the gas is given by Henry's law

$$P = K_H \bar{X} \quad (7)$$

where P is the partial pressure of the gas, K_H is Henry's law constant and \bar{X} is the mole fraction of the gas dissolved in the solvent (Ref 1: 345).

Power Output of a Laser

The power of a laser is given by

$$P_{\text{laser}} = P_{\text{fluor}} \left(\frac{R_p}{R_{\text{pth}}} - 1 \right) \quad (8)$$

where P_{fluor} is the fluorescent power, R_p is the pump rate, and R_{pth} is the threshold pumping rate.

R_{pth} is given by

$$R_{\text{pth}} = \frac{1}{K_{\text{laser}} \tau_c \tau_2} \quad (9)$$

where K_{laser} is the laser rate constant, τ_c is the photon cavity lifetime, and τ_2 is the lifetime of the upper laser level (Ref 14:394).

τ_c is given by

$$\frac{1}{\tau_c} = \ln \frac{1}{r_1 r_2} \quad (10)$$

where r_1 and r_2 are the reflectivities of the mirrors (Ref 14:424-428).

III. Apparatus

The equipment used in this project is placed in three groups depending on usage.

Continuous Radiation Photolysis System

The photolysis system shown in Fig. 3 consists of three basic parts: a source of light, a container for the dye and a source of gas.

The light source is a 200 watt Osram HBO 200 mercury point source whose line spectra is shown in Fig. 4. The lamp is housed in a Bausch and Lomb lamp housing and is powered by an Oriol 8500 power supply. The lamp housing contains a quartz condenser lens system. The light from the lamp passes out of the lamp housing and into the dye container housing through a quartz cell used to hold the filter liquid. To keep the filter from evaporating a small siphon from a flask is used to keep the cell full.

The dye container, shown in Fig. 5 consists of 21.5 cm long by 2.5 cm in diameter pyrex and quartz cylinder whose bottom 6 cm is quartz. At the top of the cylinder is a ground glass joint and near the top extending out at an angle is a septum. The dye container housing is a rectangular cube with a hole in the top through which the dye container is inserted, and a hole in the bottom so that the bottom of the dye container can make contact with the magnetic stirrer immediately below the housing. A fan is attached to the back of the housing and holes are drilled in the front of the housing so that a flow of air can cool the dye container. A hole on one side allows light to enter and strike the lower portion of the dye container.

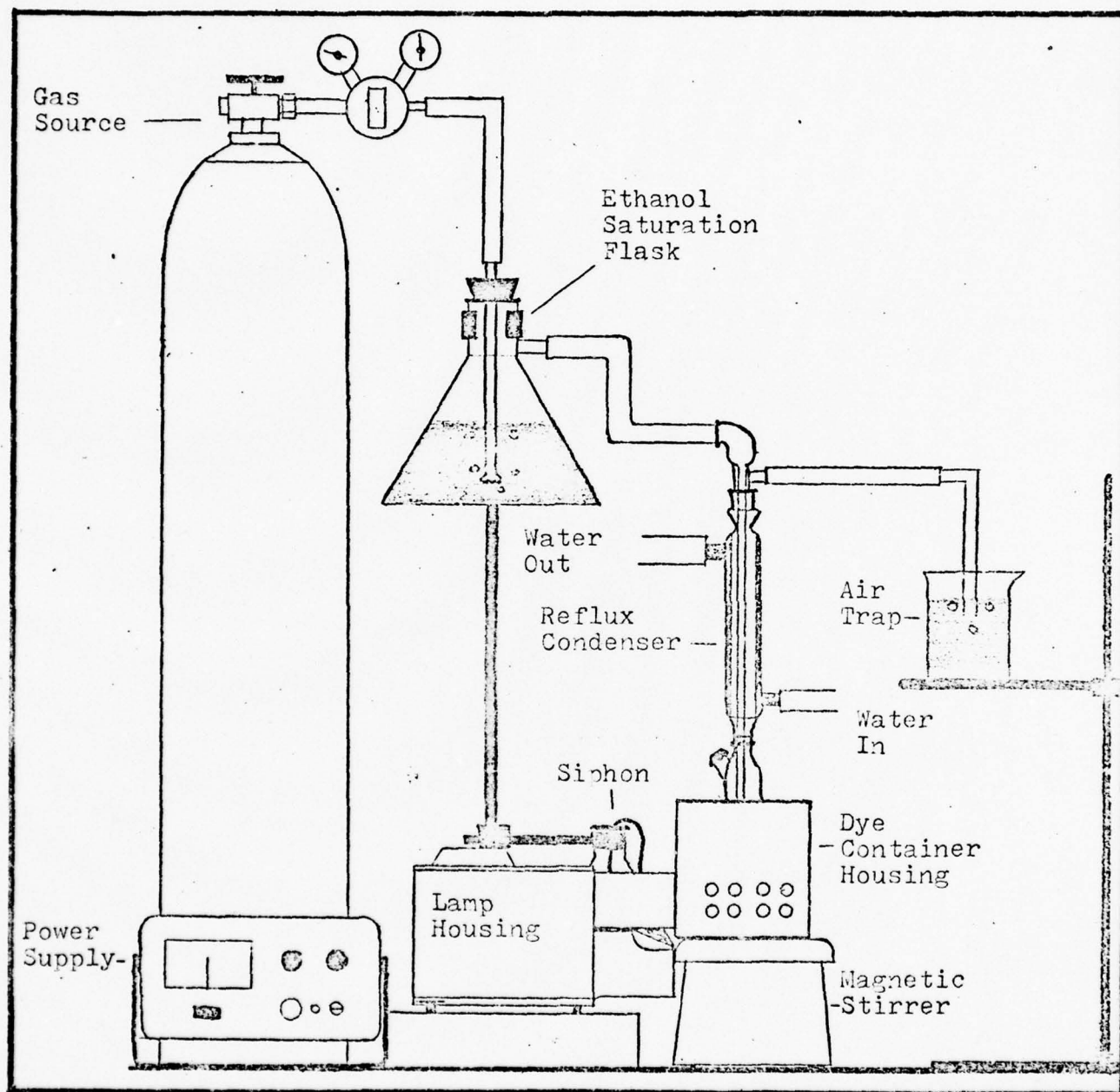


Fig. 3. The Photolysis System

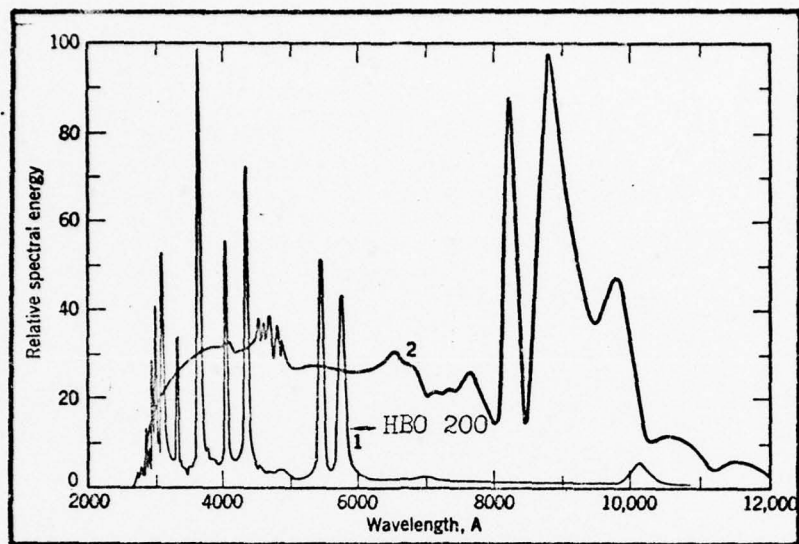


Fig. 4. Spectrum of the Lamp (From Ref 4:704)

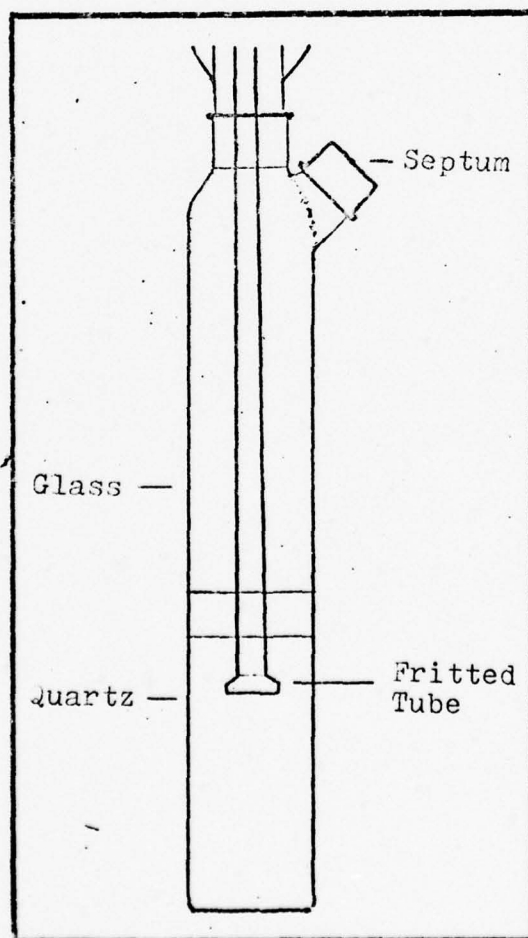


Fig. 5. The Dye Container

A small reflux condenser with a 90° adapter and side arm is fitted to the top of the dye container to help control solvent evaporation from the dye solution. The gas mixture, from a high pressure cylinder is bubbled through ethanol in a side arm flask to help prevent evaporation of the solvent from the dye solution by saturating the gas mixture with ethanol. The saturated gas mixture enters the dye container through the 90° adapter and is bubbled through the dye solution. The gas mixture leaves the dye container through the side arm on the 90° adapter. A flask filled with ethanol is used as a trap to prevent air from entering the dye container through the side arm.

Dye Laser System

The dye laser system is a Phase-R DL-1100 flash lamp pumped dye laser. The laser was converted from a biaxial to a triaxial dye laser with a Phase-R modification kit. A biaxial dye laser consists of a tube through which the dye solution flows, surrounded by a helical flash lamp. A triaxial dye laser has an extra cavity between the dye tube and the flash lamp through which a coolant flows. The coolant can also be used to filter the radiation from the flash lamp. See Fig. 6.

There are six subsystems on the laser: the laser head, the power supply and controls, the dye solution circuit, the coolant circuit, the temperature regulator, and the diagnostic equipment. See Fig. 7. The laser head is the DL 110 flash lamp with the triaxial adapter. The mirrors are flat and have reflectivities of 27 percent and 99 percent. The mirrors are mounted along with the flash lamp on top of the capacitor housing. The power supply and controls are also standard manufacture DL 1100 equipment. The temperature regulator is a Korad

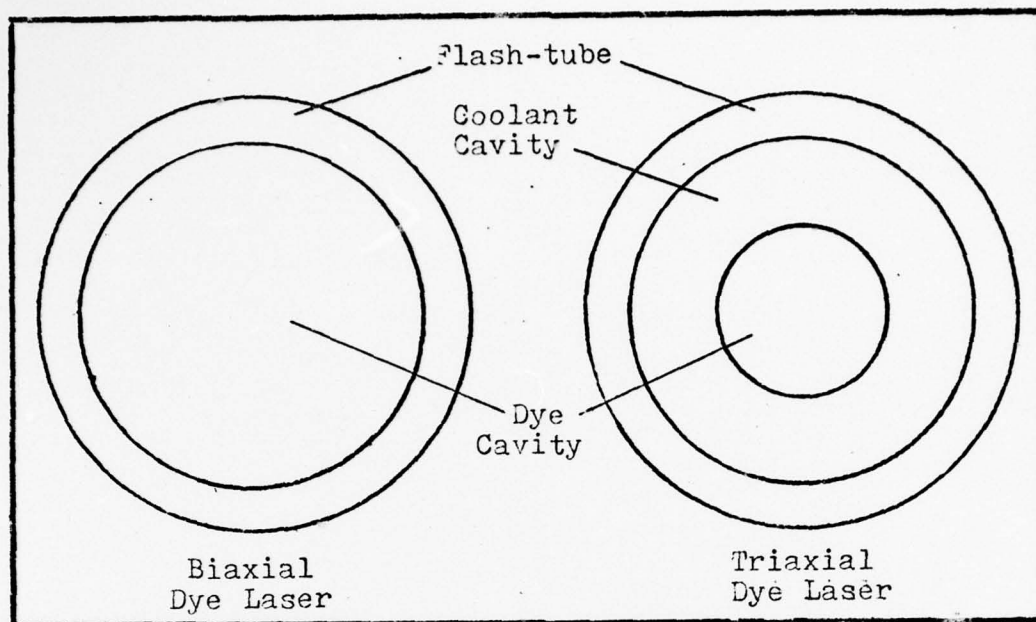


Fig. 6. Types of Lasers

KNC-5 laser cooler that pumps constant temperature water to the cooling condensers.

The dye solution circuit is as follows: Coming out of the laser head the solution flows into the pump. From the pump the solution is pumped up through a one-foot cooling condenser, through a filter and into the dye solution reservoir. The temperature of the dye solution is measured by a thermometer in the reservoir. From the reservoir the dye solution flows down through the fluorescence measuring equipment and into the laser head. The coolant circuit is as follows: After leaving the laser head the coolant is pumped up through a 1.25 ft condenser and into the coolant reservoir. The coolant flows out of the reservoir through a flow control valve and into the laser head.

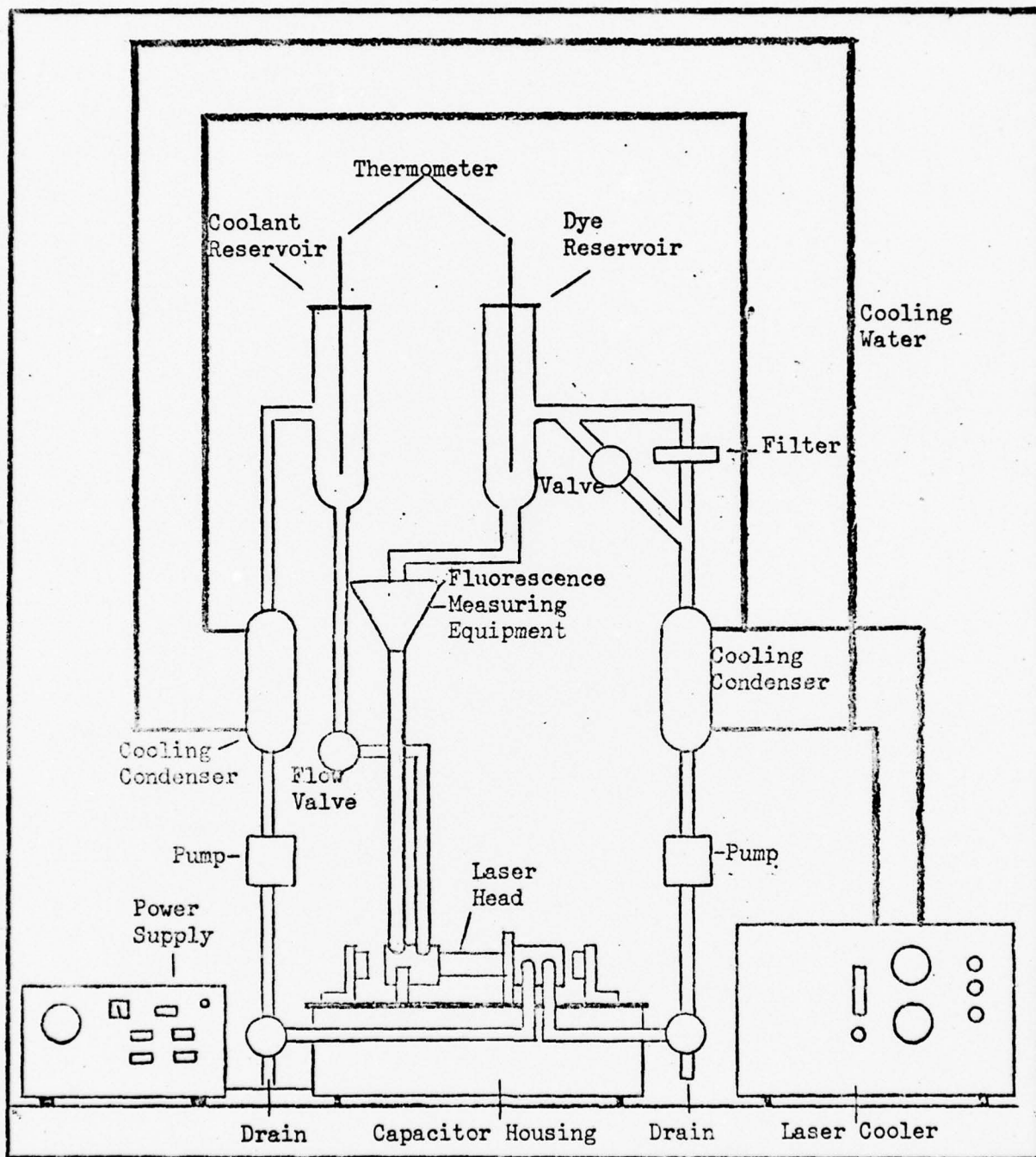


Fig. 7. Schematic of the Dye Laser

The materials used to construct the dye circuit are glass and polypropylene tubing. The dye solution pump is a March MDX-MT-3 high purity pump. The materials used to construct the coolant circuit are glass and Teflon tubing.

The diagnostic equipment consisted of a Quantronix 504 power meter and the fluorescence measuring equipment. See Fig. 8.

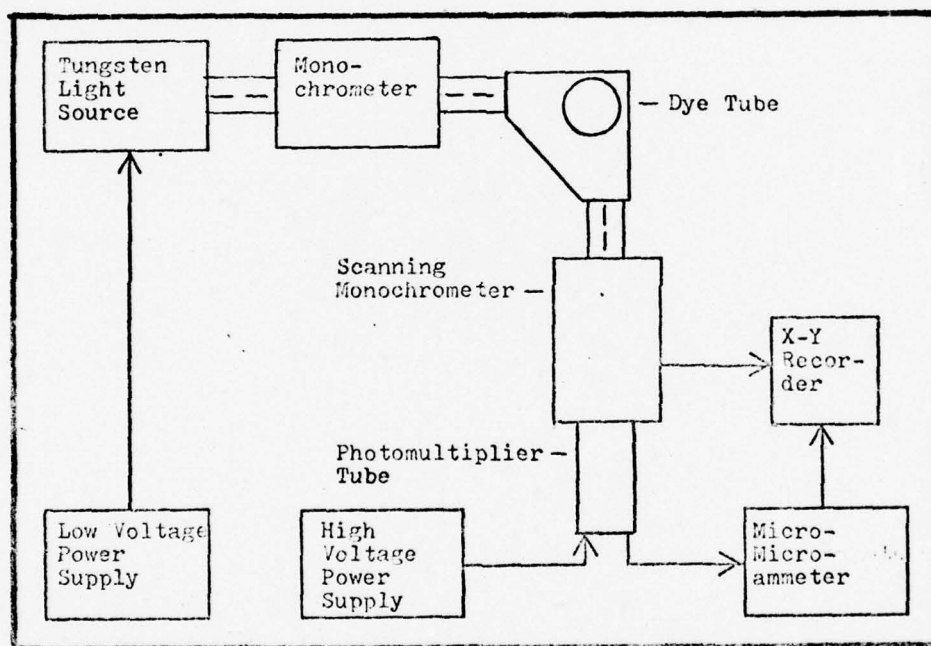


Fig. 8. Fluorescence Measuring Equipment

The fluorescence measuring equipment consists of a Bausch and Lomb tungsten light source powered by a Lambda IM-F8-OVM power supply, a Bausch and Lomb monochromometer, a Bausch and Lomb scanning monochromometer, an EMI 6255B photomultiplier tube powered by a Kepco HB 2500 high voltage power supply, a Keithley 414 micro-microammeter, and a Hewlett Packard

X-Y recorder. Monochromatic light at 500 nm produced from tungsten lamp by the monochromator is passed through the dye solution flowing in a glass tube. The fluorescence is measured with the scanning monochromator and associated electronics at a right angle from the incident light.

Analysis Equipment

The third group of equipment is that used to analyze the samples. This group includes the vacuum evaporation chamber, a Crescent Wiggle Bug dental amalgam shaker, a Crescent stainless steel amalgam capsule, a Perkin Elmer pellet dye, a Carver 20,000 lb laboratory press, a Fisher vacuum pump, and a Perkin Elmer 137 sodium chloride IR spectrometer.

The vacuum evaporating chamber is a 500 ml side arm flask that was immersed in a controlled temperature water bath. A rubber stopper fitted with a stop cock is used to control the air entering the flask. The vacuum source is an aspirator with a dry ice slurry water vapor trap. A 10 ml beaker of dessicant is placed in the flask to help hold down the humidity.

IV. Experimental Procedure

The general procedure will be described first, then modifications for each experiment will be discussed.

Continuous Radiation Photolysis

The general procedure for performing the CW photolysis experiments was as follows. Seventy-five ml of 10^{-3} M Kiton Red-S in ethanol was placed into the dye container. The system was assembled and ethanol was placed in the two flasks. The system and the dye solution were equilibrated with the gas mixture by rapidly bubbling the gas through the solution. After at least two hours of rapid bubbling the lamp was turned on and the bubbling was reduced to a moderate rate. The lamp power supply was adjusted to 34 amps of current. After the first 12 hours and after all subsequent 12-hour periods, a 1 ml sample was withdrawn with a gas tight syringe through the septum on the dye container. These samples were processed using the solid KBr pellet IR analysis discussed later. Occasionally a sample would be withdrawn for an IR analysis of the solution in a liquid cell with AgBr windows and a 0.05 mm path length.

Flash Photolysis

The procedure for performing the laser experiment was as follows. The laser was aligned according to the manufacturer's instructions, and a 5 micron millipore Teflon filter was installed in the filter holder. The laser was filled with 500 ml of 10^{-4} M KRS in ethanol. Five hundred

ml deionized water was used as the coolant. The pumps and laser cooler were turned on. The discharge water temperature of the cooler was set at 60° F and the temperature of the coolant and the dye solution was brought as close together as possible by adjusting the flow valve and observing the thermometers. The capacitor voltage used to fire the laser was 18 KV. On the initial firing the power and fluorescence spectrum was taken and after each increment of 250 shots, the power of the laser and the fluorescence spectrum was taken.

Sample Analysis

Fifteen hundredths gm of oven dried KBr was added to the stainless steel capsule along with the 1 ml of dye solution taken from the continuous radiation photolysis apparatus. The capsule was placed in a 5 ml beaker for support, and the capsule and beaker were placed in the evaporating chamber. The chamber was evacuated and the temperature of the water bath was brought up to and maintained at 30° C. After the ethanol had completely evaporated, air was reintroduced into the chamber and the capsule was removed. A steel ball bearing was placed in the capsule and the capsule was capped. The capsule was shaken for one minute on the Wiggle Bug and a sample 0.10 gm of the resulting powder was weighed out and placed in a dessicator to dry for at least eight hours. The powder was then placed in the pellet die. The die was assembled and evacuated with the vacuum pump. The pellet was pressed at 20,000 lb for one minute, then the vacuum was released slowly, and the pressure was removed. The pellet was removed from the die and placed in a holder. The holder was attached to the IR spectrometer and the spectrum was made using a

15-minute scan with the slits on N. The base line of the spectrum was arranged so that it would fall at 95 percent transmittance.

Experimental Details

A calibration curve of the IR absorption intensity versus dye concentration was made using a series of solutions with concentrations from 1×10^{-4} M to 10×10^{-4} M. These samples were analyzed in the same manner as the samples taken during the CW photolysis experiment. This curve was used to find the concentration of KRS remaining in a sample after degradation.

The first trial of the CW photolysis experiment was designed to establish a base line for the kinetic analysis of the rest of the experiment. In order to eliminate oxygen from the dye solution pure argon was bubbled through the solution. The filter cell was empty. After the dye solution had been exposed a sufficient amount of time (144 hours) to establish a base line, air was bubbled through the solution to establish if oxygen has an effect on the kinetics. The remaining two trials were done to find the effect of different oxygen concentrations on the kinetics of the reaction as well as to test the effect of a filter.

The second trial was done with 10.3 percent oxygen in argon bubbled through the solution, and the third trial was done with air (21 percent oxygen). After 156 hours exposure in the third trial the filter cell was filled with ethanol to see if the kinetics would show if ethanol was the primary photoprocess by filtering out the wave lengths of light that excite ethanol.

The laser experiment was done exactly as described.

V. Data Reduction

The raw data for each of the CW photolysis trials consisted of a set of IR spectrograms. The data was reduced in five steps: the appropriate peak was selected for measurement, the size of the peak was measured, the concentration of KRS in solution was determined, the concentration of KRS versus time of exposure was plotted, and the appropriate parameters for the resulting curves were calculated.

The peak that was chosen was a strong peak at 7.5 microns. It was observed that the disappearance of that peak is representative of the disappearance of the entire IR spectrum of Kiton Red-S, and there was no interference with this peak by the spectrum of reaction products. This peak was also chosen because a stable tie line could be drawn for this peak. See Fig. 10.

The size of the peak was calculated by measuring the absorbance A at the bottom of the peak and subtracting it from the absorbance A_0 at the tie line. Since most of the spectra were made with the Y axis measured in percent transmission, the percent transmission was converted to absorbance by overlaying the two scales.

To determine the concentration of KRS in solution, the calibration curve was used to read the concentration of KRS from the size of the peak (Ref 6:182-195). The Y intercept of each of the curves for the experimental trials was not 10×10^{-4} M because a different batch of dye solution was used for each trial. A correction factor was required to normalize each curve to 10×10^{-4} M initial concentration. A sample is given in Appendix A.

From the laser experiment the raw data was a set of fluorescence spectra of KRS in ethanol. See Fig. 9. The height of the fluorescence peak was measured in centimeters from the base line to the top of the peak. This height was proportional to fluorescence power.

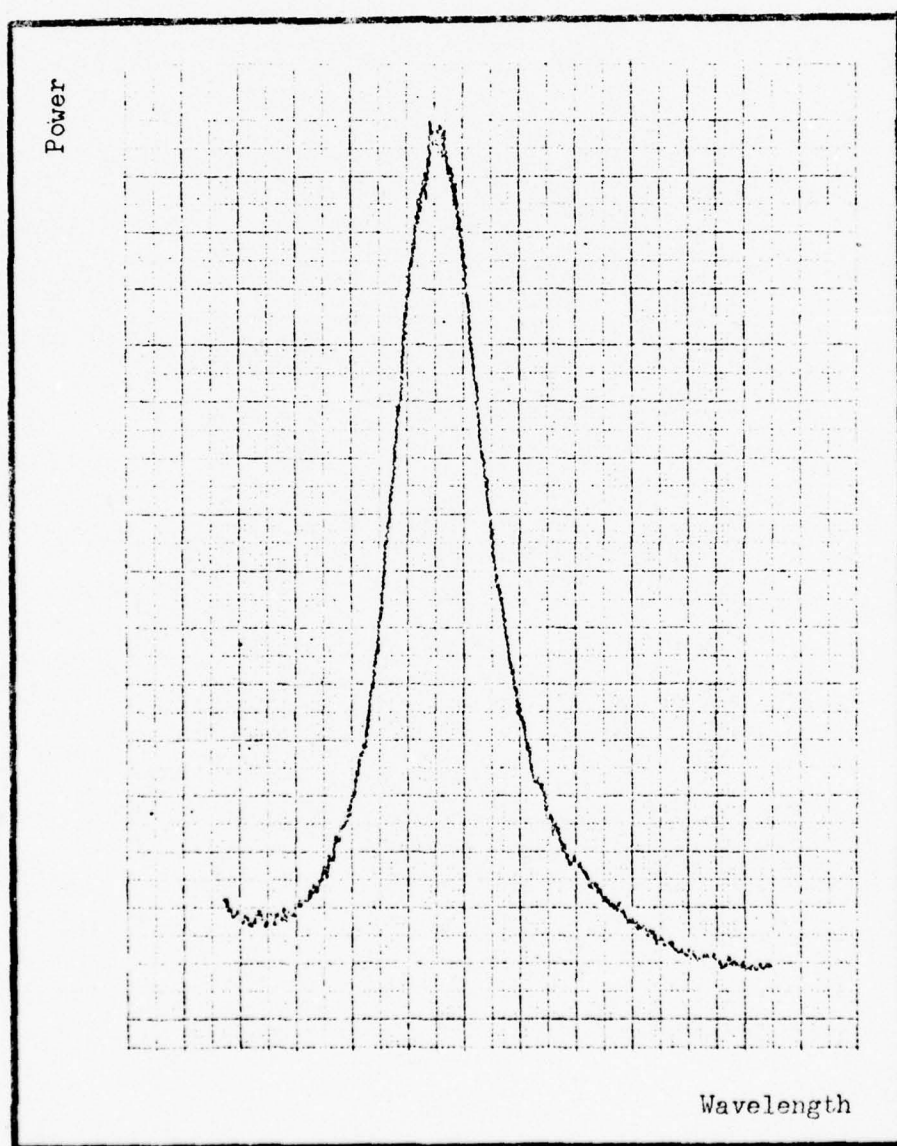


Fig. 9. Fluorescence of Kiton Red-S

VI. Results

Qualitative Results

The IR spectrum of the unexposed KRS is given in Fig. 10, and the IR spectrum of the KRS degraded in the CW photolysis experiment is given in Fig. 11. A possible assignment of some of the bands of both spectra is given in Table I. The most important points in comparing the two spectra are as follows:

1. The growth of the bands at 3 microns, 5.75 microns, 6.00 microns, 7.25 microns, 8.25 microns, 9.00 microns and 9.75 microns.
2. The stability of the bands at 9.75 microns, 3.25 microns, and 14.25 microns.
3. The disappearance of the bands at 3.50 microns, 6.25 microns, 6.75 microns, 7.25 microns, 7.50 microns, 7.75 microns, 8.75 microns, 9.25 microns, 10.25 microns, 10.75 microns, 12.25 microns, and 14.75 microns.

The IR spectrum of the degraded solution using the liquid sample cell shows some of the degradation products that are present in the samples processed using KBr pellet analysis. The spectrum of both the KRS and the degradation products is so weak compared to the spectra of the ethanol that the technique was not used. There is a strong fruity smell in the degraded samples.

Quantitative Results

Fig. 12 shows the calibration curve for IR absorbance versus KRS concentration in ethanol. A least squares analysis of the data produced

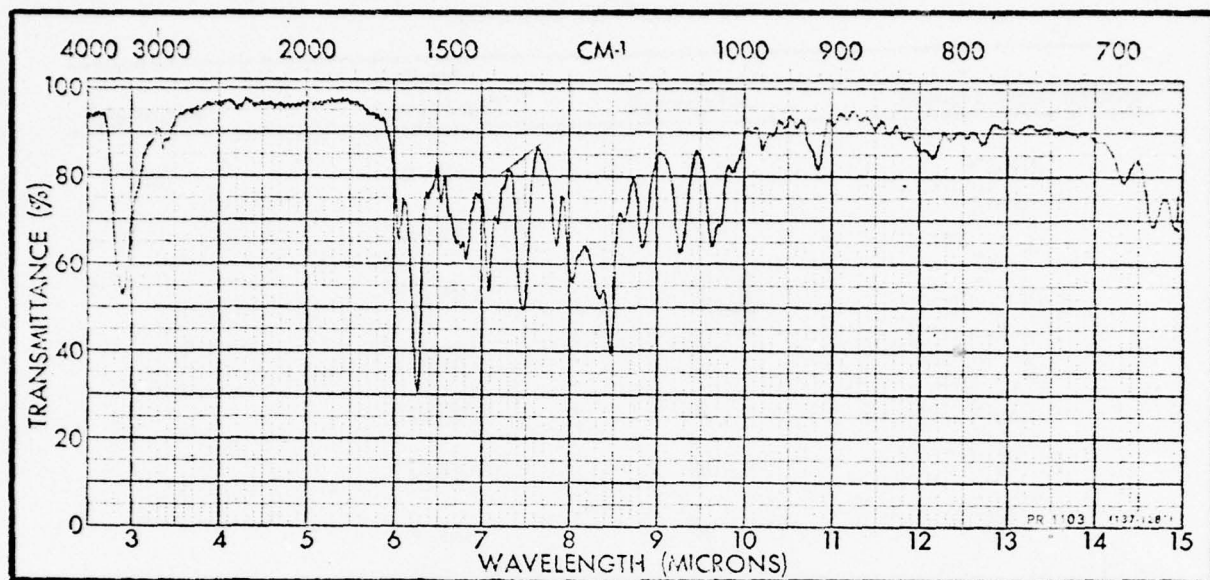


Fig. 10. IR Spectrum of Kiton Red-S

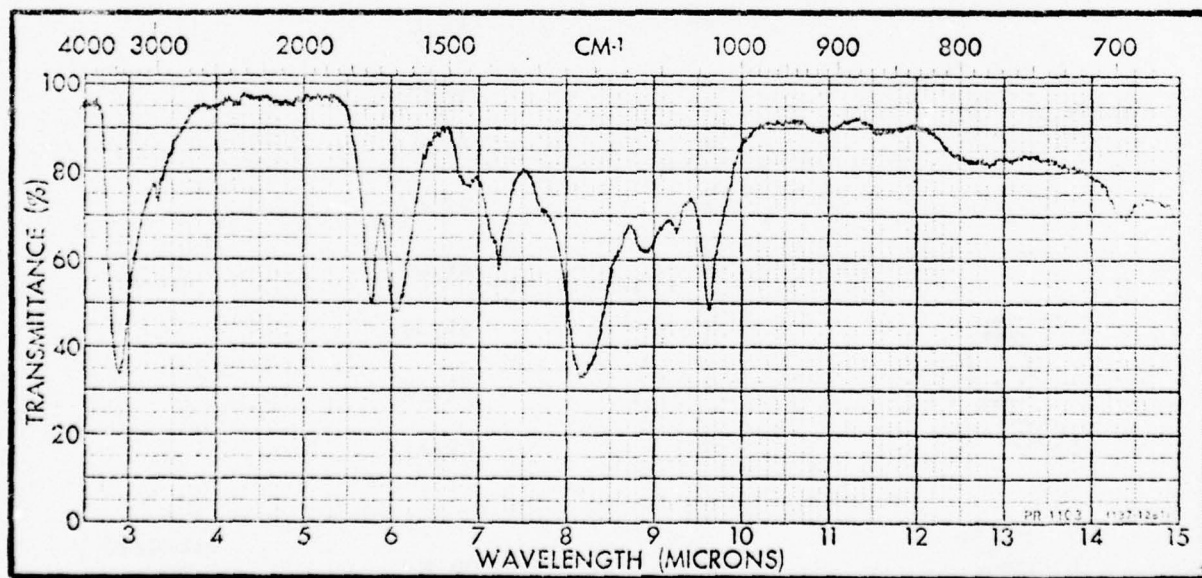


Fig. 11. IR Spectrum of Degraded Kiton Red-S

Table I
Infrared Assignments







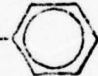
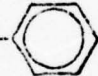






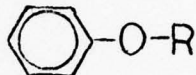
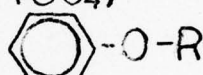

Spectrum	Band (microns)	Strength	Functional Group
KRS	3.00	S	-OH
	3.25	W	- 
	3.50	W	-C ₂ H ₅
	6.00	M	- 
	6.25	S	-C ₂ H ₅
	6.75	M	-C ₂ H ₅
	7.00	M	- 
	7.50	S	-  -NR ₂
	7.75	M	- 
	8.00	M	-  -NR ₂
	8.25	M	-  -O-R
	8.50	S	R-SO ₃
	8.75	M	- 
	9.25	M	R-SO ₃
	9.75	M	-  -O-R
	10.25	W	- 
	10.75	W	- 
	12.25	W	- 
	14.25	M	- 
	14.75	M	R-SO ₃
Degraded KRS	3.00	S	-OH
	3.25	M	- 
	5.75	S	R-CO-O-R

Table I (continued)
Infrared Assignments

Spectrum	Band (microns)	Strength	Functional Group
Degraded KRS	6.00	S	-CO-OH
	6.75	W	—
	7.25	M	-CO-OH
	8.25	S	R-CO-O-R, -CO-OH,
			
	8.75	M	(SO ₄) ⁻⁻⁻
	9.75	S	
	14.25	M	

(Ref 17; F-197-F-203)

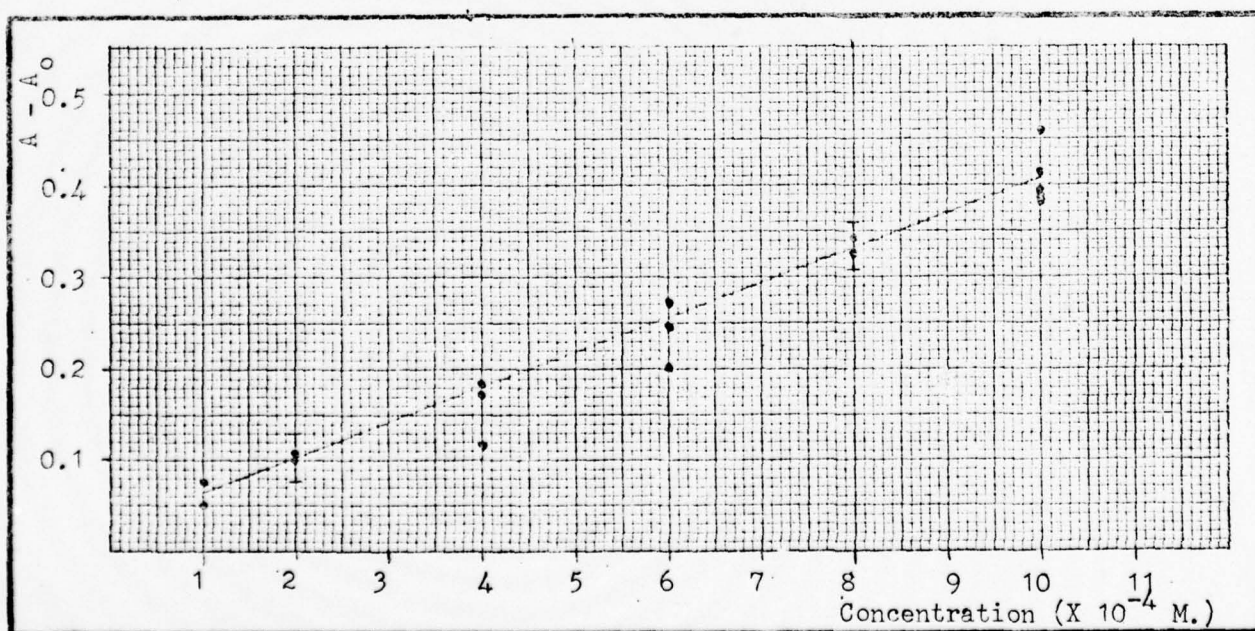


Fig. 12. Calibration Curve

the straight line which is shown. The standard deviation of the points is 0.025. The linearity of the curve indicates that the Beer Lambert law holds over the range of concentrations used.

The results of the first trial of the CW photolysis experiment are shown in Fig. 13. A least squares analysis of the data produced the straight line shown. No line is drawn through the data points after air exposure since the experiment was not rigorous after that point. The slope of the line is -0.0052 mole/liter hour with a standard deviation of the points of 0.83. The correlation coefficient is a measure of how well the independent variable of a plot depends on the dependent variable. The coefficient ranges from 0 (no dependence) to one (perfect dependence). The correlation coefficient for the first trial is 0.28.

The results of the second trial are shown in Fig. 14. A least squares analysis produced the straight line shown. The slope of the line is -0.043 moles/liter hour with a standard deviation of the points of 0.65. The correlation coefficient is 0.97.

The results for the third trial are shown in Fig. 15. A straight line was also obtained from a least squares analysis. The slope of the line is -0.054 mole/liter hour with a standard deviation of the points of 0.45. The correlation coefficient is 0.98. To show the effect of the ethanol filter the difference in the absorbance was plotted versus time in Fig. 15. The difference was not converted to concentration since the value of some of the points was beyond the range of the calibration curve. All the raw data is given in tabular form in Appendix B.

There is a large increase observed in the amount of time it takes to obtain visual bleaching of the dye solution when bubbling is taking place. Previous experiments performed at the Air Force Avionics

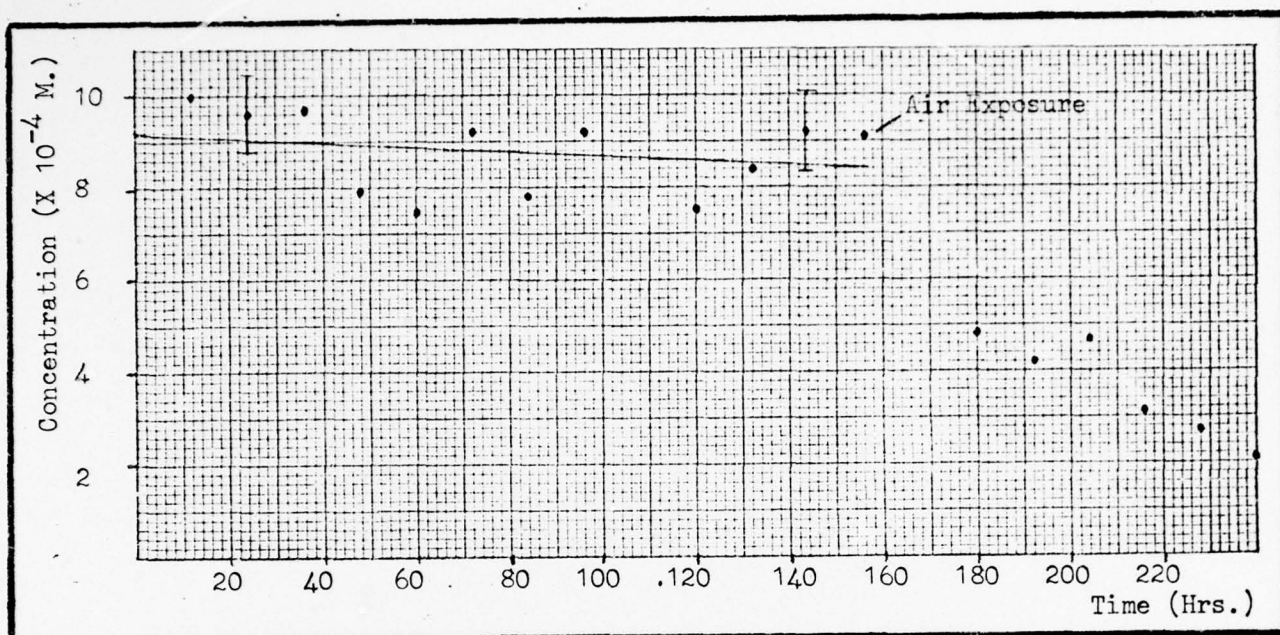


Fig. 13. Degradation of KRS, Zero Oxygen

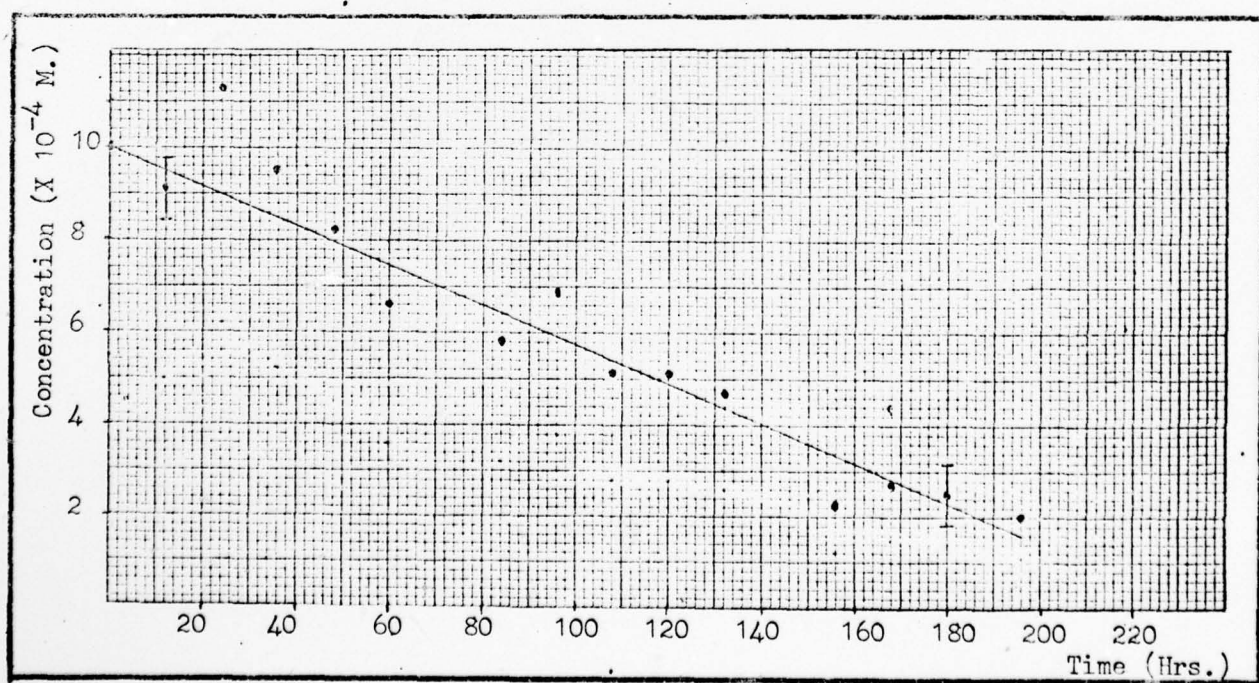


Fig. 14. Degradation of KRS, 10.3 Percent Oxygen

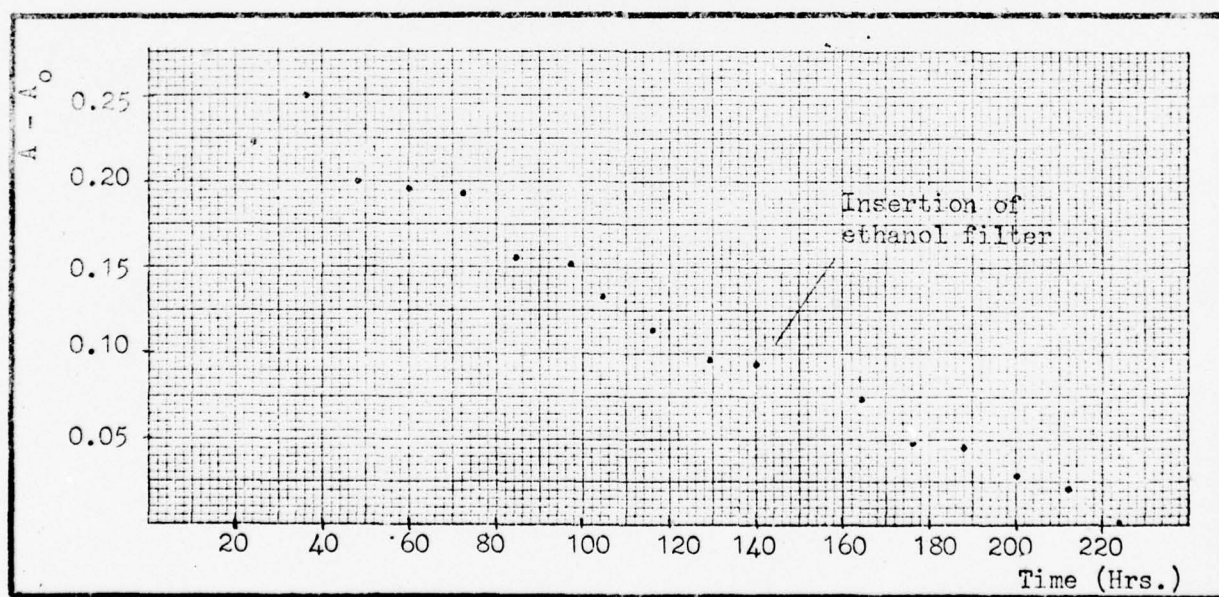
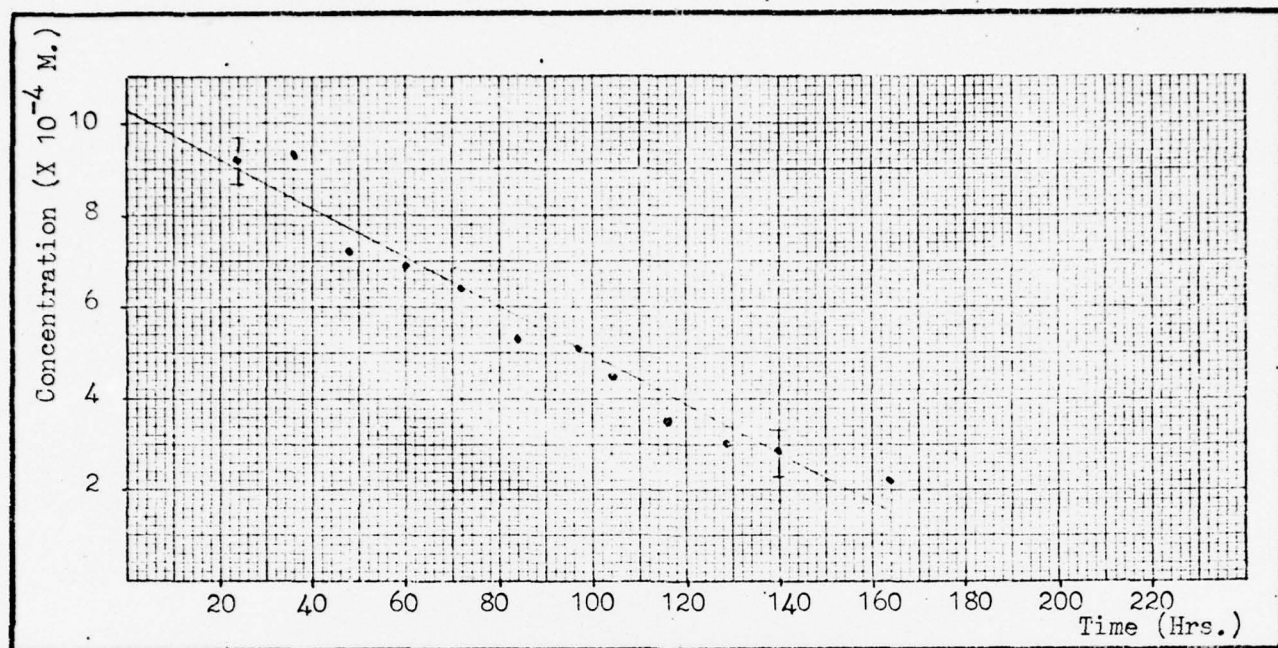


Fig. 15. Degradation of KRS, 21 Percent Oxygen

Laboratory with the same CW photolysis equipment but without bubbling showed bleaching occurred in about 60 hours. Results from this experiment with bubbling show that visual bleaching occurs in over 250 hours.

The results from the laser experiment show that for a 4 percent decrease in fluorescence power, there is an 84 percent decrease in the output power of the laser.

VII. Discussion

Discussion of CW Photolysis Results

The disappearance of the 3.50 micron, 6.75 micron and the 7.00 micron bands tends to indicate a change in or loss of the ethyl groups on the KRS molecule. The disappearance of the 7.50 micron band also indicates attack on this site since the 7.50 micron band represents the tertiary amine to which the ethyl groups are attached. The disappearance of the 9.25 and the 14.75 micron bands indicates that the sulphate groups are attacked. The sulphate groups might be breaking off to form an inorganic sulphate salt as there is an increase in water (3 micron band) in the sample and there is the growth of a band of 9 microns which corresponds to inorganic sulphates. There is the possibility of the loss of an aromatic portion of the molecule since the aromatic band at 6.25 microns disappears but the aromatic bands at 3.25 microns and 14.25 microns are stable. The portion that is lost is probably the phenyl group to which the sulphates are attached. The stability of the band at 9.75 microns indicates that the aromatic ether at the center of the KRS molecule remains relatively intact.

The growth of the bands at 6.00 microns, 7.25 microns and 8.25 microns indicates the presence of a carboxylic acid as a degradation product. The growth of the bands at 5.75 microns and 8.25 microns indicates that another degradation product is an organic ester. This observation is strengthened by the pleasant fruity smell of the product mixture. The pleasant smell is an almost universal characteristic of organic esters.

The reaction for the CW photolysis of Kiton Red-S is zeroth order since the plot of the concentration of KRS versus time of exposure is linear. This is typical of photochemical reactions in which all of the radiation is absorbed by the reacting species (Ref 1:624). The kinetics of the reaction *does* depend on the concentration of oxygen. This oxygen dependence is shown by the marked change in the curve made during the first trial when air was introduced, and by the large increase in the correlation coefficient from 0.28 to about 0.98 when oxygen is present. Oxygen accelerates the reaction. The experimentally determined rate equation is

$$\frac{d [KRS]}{dt} = -k [KRS]^0 [O_2]^a \quad (11)$$

where k is the actual rate constant. k may contain dependencies on other factors which are unknown. The apparent rate constant, K , which is equal to the slopes measured in the three trials, includes the concentration of oxygen as shown.

$$\frac{d [KRS]}{dt} = K [KRS]^0 \quad (12)$$

where

$$K = k [O_2]^a \quad (13)$$

The rate constant, k , and a can be calculated from the data. The concentration of oxygen in solution is calculated using Henry's law, with Henry's law constant, K_H calculated from the International Critical Tables (Ref 16:255-282). The values for K and $[O_2]$ are known or calculated for two points and solving Eq (13) at the two points simultaneously

yields k and a . The amount of oxygen dissolved in solution is assumed to be constant over each trial. The values of the apparent rate constant k , the percent oxygen in the gas mixture, the concentration of oxygen in solution and the correlation coefficient are given in Table II. The calculated value for k is 1.0×10^{-4} and the calculated value for a is 0.31. The rate equation can now be written as

$$\frac{d [KRS]}{dt} = 1.0 \times 10^{-4} [KRS]^0 [O_2]^{0.31} \quad (14)$$

The large increase in the amount of time it takes for visual bleaching to occur when gas is bubbling through the solution suggests the possibility of some volatile intermediate which is necessary for the continuation of the reaction. This intermediate is removed by the bubbling. The lack of any significant change in slope in the third trial upon insertion of ethanol into the filter cell tends to rule out the direct excitation of ethanol by the light as a primary photoprocess. This result may not be significant since the filter cell had a very small path length (1 mm) and some of the lines that excite ethanol might have been passed.

Bringing all this evidence together, a possible reaction mechanism may be proposed. Since the reaction is zeroth order in KRS, the dye is not a factor in its own degradation, except perhaps as a catalyst. Since the concentration of oxygen does have a power dependence, oxygen does have a part in the degradation as a reactant. Since the direct excitation of ethanol by the light has been ruled out, the light must be

exciting the dye. The dye then passes the energy to the ethanol solvent. The solvent breaks up to yield a volatile and highly reactive intermediate which along with the oxygen attacks the dye molecules. This causes destruction of the dye's functional groups, and the creation of oxidation products such as esters and carboxylic acids.

Table II
Numerical Results

	Percent Oxygen in Trial Gas Mixture	Concentration of Oxygen in Solution (Mole/liter)	Apparent Rate Constant (Mole/liter sec)	Correlation Coefficient
One	0	0	-1.4×10^{-6}	0.28
Two	10.3	9.9×10^{-4}	-1.2×10^{-5}	0.97
Three	21	2.0×10^{-3}	-1.5×10^{-5}	0.98

Discussion of Laser Results

As can be seen from Eq (8), a four percent decrease in fluorescent power can not account for the 84 percent decrease in output power. This large decrease can only be accounted for by a decrease in R_p . It is probable that the reaction products are absorbing the pump radiation.

VIII. Conclusions

1. The photolytic reaction in the continuous radiation experiment is zeroth order in Kiton Red-S.
2. The reaction rate in the continuous radiation experiment is increased with increased oxygen concentration.
3. Among the products present in the bleached solution from the continuous radiation experiment is a carboxylic acid and an organic ester.
4. There may be a volatile necessary intermediate in the continuous radiation photoprocess.
5. The primary effect of the photo products on the laser is to absorb the pump radiation.

IX. Recommendations

1. The KBr pellet method must be further refined.
2. The effect of oxygen on the degradation must be isolated.
3. The effect of the wavelength of the pump radiation on degradation must be isolated.
4. Samples from the laser must be analyzed using the KBr pellet/IR spectroscopy technique.
5. The results from the continuous radiation experiment must be extended to the laser.

Bibliography

1. Addamson, A. W. A Textbook of Physical Chemistry. New York: Academic Press, 1973.
2. Allenger, N. L., et al. Organic Chemistry. New York: Worth Publishing Co., 1971.
3. Beer, D. and J. Weber. "Photobleaching of Organic Laser Dyes." Optics Communications, 5: 307-309 (July 1972).
4. Calvert, J. G. and J. N. Pitts, Jr. Biochemistry. New York: John Wiley and Sons Inc. (1967).
5. Drexhage, K. H. "Structure and Properties of Laser Dyes" in Topics in Applied Physics, Dye Lasers, edited by F. P. Schafer. New York: Springer-Verlag (1973).
6. Fritz, J. S. and G. S. Hammond. Quantitative Organic Analysis. New York: John Wiley and Sons Inc. (1957).
7. Hewlett-Packard H-P 25 Applications Programs. Hewlett-Packard Co. (1975).
8. Ippen, E. D., et al. "Rapid Photobleaching of Organic Laser Dyes in Continuously Operated Devices." IEEE Journal of Quantum Electronics, pp. 178-179.
9. Kato, D. and A. Sugimura. "Deterioration of Rhodamine 6 G Dye Solution in Methanol." Optics Communications, 10: 327-330 (April 1974).
10. McCracken, D. D. A Guide to Fortran IV Programming. New York: John Wiley and Sons Inc. (1972).
11. Mostovnikov, V. A., et al. "Recovery Lasing Properties of Dye Solutions After Their Photolysis." Soviet Journal of Quantum Electronics, 6: 1126-1128 (September 1976).
12. Neister, E. S. "The Dye Laser Dye Update." Optical Spectra, pp. 34-36 (February 1977).
13. Shank, C. V. "Physics of Dye Lasers." Reviews of Modern Physics, 47: 649-657 (July 1975).
14. Siegman, A. E. An Introduction to Lasers and Masers. New York: McGraw-Hill Book Co., 1971.

15. Warden, J. T. "Flashlamp-Pumped Laser Dyes: A Literature Survey." Applied Physics Letters, 19: 345-348 (November 1971).
16. Washburn, E. W., ed. International Critical Tables of Numerical Data, Physics, Chemistry, and Technology, III. New York: McGraw-Hill Book Co. (1928).
17. Weast, R. C., ed. Handbook of Chemistry and Physics. 53rd edition, Cleveland, Ohio: The Chemical Rubber Co. (1972).
18. Weber, J. "Continuously UV-Bleaching of Organic Laser Dyes." Physics Letters, 45A: 35-36 (August 1973).
19. Winters, B. H., et al. "Photochemical Products in Coumarin Laser Dyes." Applied Physics Letters, 25: 723-725 (December 1974).
20. Yamashita, Miko and Hiroshi Kashiwagi. "Photodegradation Mechanisms in Laser Dyes: A Laser Irradiated ESR Study." IEEE Journal of Quantum Electronics, 12 (February 1976).

Appendix A

Sample Calculation

Sample Calculation

As shown in Fig. 16 a tie line is drawn between the peak at 7.5 microns. The value of the transmittance at the bottom of the peak is 51 percent. This transmittance is converted into absorbance by using the scale in Fig. 17. As can be seen, 51 percent is equivalent to 0.090 on the absorbance scale. The value of the transmittance at the tie line over the bottom of the peak is 83 percent. The equivalent absorbance is 0.290. The difference $A - A_0$ is 0.200. The concentration of KRS is read off the calibration curve from $A - A_0$. The concentration of KRS is 4.5×10^{-4} M. This concentration is multiplied by the normalization factor to obtain the normalized concentration. The normalized concentration is 8.2×10^{-4} M. This procedure is done for all the IR spectra in the run. The normalized concentration is plotted against the time of exposure. A straight line is fitted to the data using least squares and the slope of the line is calculated. The coefficient of determination, r^2 , is calculated (Ref 7:87-89). The coefficient of correlation, r , is then calculated (Ref 10:82).

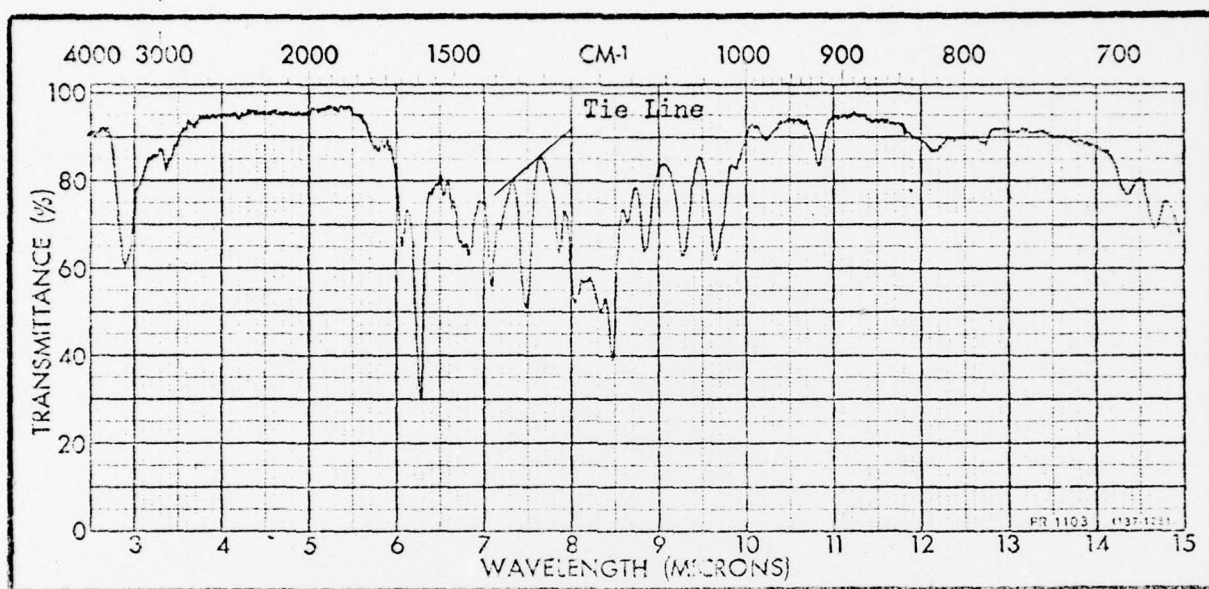


Fig. 16. IR Spectrum of Partially Degraded Kiton Red-S

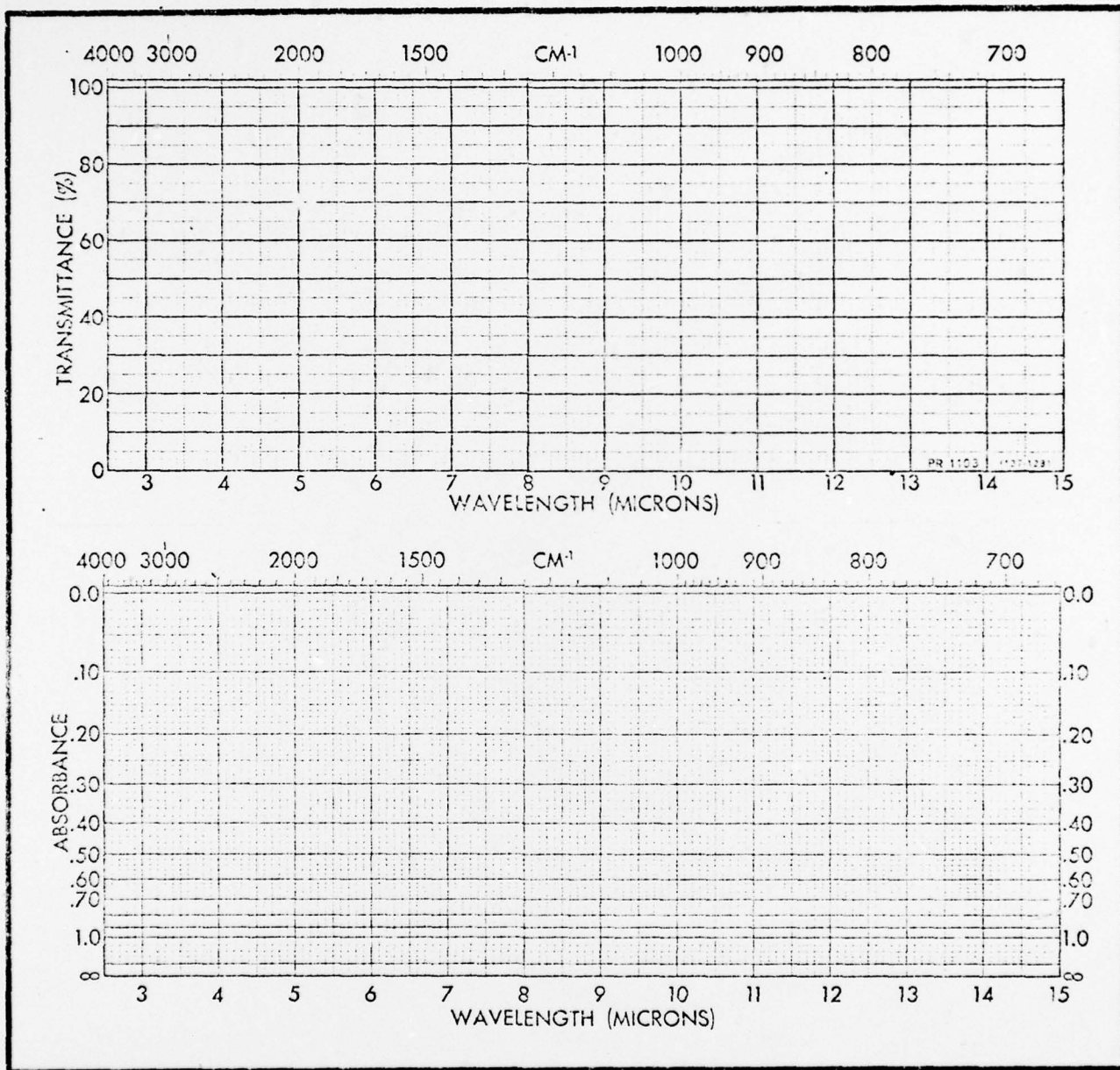


Fig. 17. Conversion Scale for Transmittance to Absorbance

Appendix B

Tabular Data

Table III
Data from the Calibration Curve

Concentration ($\times 10^{-4}$ M)	A_0	A	$A - A_0$
10	0.098	0.495	0.397
10	0.140	0.600	0.460
10	0.113	0.505	0.392
10	0.109	0.490	0.381
10	0.092	0.505	0.413
10	0.109	0.495	0.386
10	0.102	0.495	0.393
1	0.042	0.092	0.050
2	0.061	0.169	0.108
4	0.070	0.243	0.173
6	0.092	0.365	0.273
8	0.113	0.455	0.342
1	0.037	0.113	0.076
2	0.060	0.161	0.101
4	0.051	0.167	0.116
6	0.076	0.276	0.200
8	0.092	0.419	0.327
4	0.070	0.252	0.182
6	0.081	0.335	0.247

Table IV
Data from First Trial

t (hrs)	A_0	A	$A - A_0$	$C(X10^{-4} M)$	Normalized $C(X10^{-4} M)$
12	0.114	0.440	0.326	7.7	10.0
24	0.091	0.400	0.309	7.4	9.6
36	0.098	0.410	0.312	7.5	9.7
48	0.098	0.360	0.262	6.1	7.9
60	0.091	0.345	0.245	5.7	7.4
72	0.102	0.400	0.298	7.1	9.2
84	0.091	0.345	0.254	6.0	7.8
96	0.102	0.400	0.298	7.1	7.2
120	0.077	0.325	0.248	5.8	7.5
132	0.109	0.385	0.276	6.5	8.4
144	0.098	0.400	0.302	7.1	9.2
156	0.125	0.420	0.295	7.0	9.1
180	0.112	0.280	0.168	3.7	4.8
192	0.096	0.250	0.154	3.4	4.4
204	0.125	0.290	0.135	3.6	4.7
216	0.125	0.243	0.118	2.4	3.1
228	0.125	0.230	0.105	2.1	2.7
240	0.091	0.180	0.089	1.6	2.1
252	0.129	0.213	0.084	1.5	1.9

Table V
Data from Trial Two

t(hrs)	A ₀	A	A - A ₀	Concentration (X10 ⁻⁴ M)	Normalized Concentration (X10 ⁻⁴ M)
0	0.076	0.315	0.239	5.5	10.0
12	0.080	0.300	0.220	5.0	9.1
24	0.096	0.360	0.264	6.2	11.3
36	0.087	0.315	0.225	5.2	9.5
48	0.090	0.290	0.200	4.5	8.2
60	0.096	0.290	0.164	3.6	6.6
84	0.087	0.237	0.150	3.2	5.8
96	0.120	0.292	0.172	3.8	6.9
108	0.102	0.237	0.135	2.8	5.1
120	0.092	0.228	0.136	2.8	5.1
132	0.108	0.237	0.129	2.6	4.7
144	0.096	0.150	0.078	1.3	1.4
156	0.070	0.142	0.072	1.2	2.2
168	0.102	0.186	0.084	1.5	2.7
180	0.112	0.186	0.074	1.4	2.5
196	0.090	0.160	0.070	1.1	2.0

Table VI
Data from Trial Three

t (hrs)	A_0	A	$A - A_0$	Concentration ($\times 10^{-4}$ M)	Normalized Concentration C ($\times 10^{-4}$ M)
24	0.080	0.325	0.245	5.7	9.2
36	0.085	0.335	0.250	5.8	9.3
48	0.074	0.273	0.199	4.5	7.2
60	0.108	0.300	0.192	4.3	6.9
72	0.123	0.305	0.182	4.0	6.4
84	0.108	0.263	0.155	3.3	5.3
97	0.112	0.265	0.153	3.2	5.1
104	0.086	0.220	0.134	2.8	4.5
116	0.107	0.220	0.113	2.2	3.5
129	0.096	0.192	0.096	1.9	3.0
140	0.119	0.213	0.094	1.8	2.9
164	0.160	0.234	0.074	1.4	2.2
176	0.100	0.149	0.049		
184	0.095	0.140	0.045		
200	0.080	0.108	0.028		
212	0.086	0.108	0.022		

VITA

Kevin O'Brien was born on 17 October 1953 in New York, New York, son of Laurence and Mildred O'Brien. He graduated from Rockville High School in June 1972 in Vernon, Connecticut. In May 1976 he received a Bachelor of Science degree in Biophysics and was commissioned a Second Lieutenant in the United States Air Force through ROTC. He entered the Graduate Engineering Physics Program in the Air Force Institute of Technology in August 1976.

Permanent address: 66 Echo Drive
Vernon, Connecticut 06066

This thesis was typed by Mrs. Frances Jarnagin.